NASA TECHNICAL MEMORANDUM

NASA TM X-52250

GPO PRICE $ _____

CFSTI PRICE(S) $ _____

Hard copy (HC) 2.00

Microfiche (MF) .50

ff 653 July 65

NASA TM X-52250

FACILITY FORM 602

N67 11333 (ACCESSION NUMBER) — (THRU) 1

38 (PAGES) — (CODE) 03

TMX-52250 (NASA CR OR TMX OR AD NUMBER) — (CATEGORY)

DEVELOPMENT OF HIGH SPEED FLUERIC LOGIC CIRCUITRY FOR A NOVEL PNEUMATIC STEPPING MOTOR

by William S. Griffin and William C. Cooley
Lewis Research Center
Cleveland, Ohio

TECHNICAL PAPER proposed for presentation at Symposium on Fluidics sponsored by the American Society of Mechanical Engineers and the Harry Diamond Laboratories
Lafayette, Indiana, May 8-10, 1967

NATIONAL AERONAUTICS AND SPACE ADMINISTRATION · WASHINGTON, D.C. · 1966

DEVELOPMENT OF HIGH SPEED FLUERIC LOGIC CIRCUITRY FOR A NOVEL PNEUMATIC STEPPING MOTOR

by William S. Griffin and William C. Cooley

Lewis Research Center
Cleveland, Ohio

TECHNICAL PAPER proposed for presentation at

Symposium on Fluidics
sponsored by the American Society of Mechanical Engineers
and the Harry Diamond Laboratories
Lafayette, Indiana, May 8-10, 1967

NATIONAL AERONAUTICS AND SPACE ADMINISTRATION

DEVELOPMENT OF HIGH SPEED FLUERIC LOGIC CIRCUITRY FOR FOR A NOVEL PNEUMATIC STEPPING MOTOR

by William S. Griffin and William C. Cooley

Lewis Research Center
National Aeronautics and Space Administration
Cleveland, Ohio

ABSTRACT

Under a NASA-Lewis Research Center program aimed at nuclear rocket control drum actuator improvement, a novel, pneumatic stepping motor has been developed. This paper describes improved, NASA-developed high speed flueric logic circuitry to drive the motor, the breadboard performance of the logic circuitry-stepping motor system, and finally compares the pneumatic stepping motor actuation system with the more conventional pneumatic piston-in-cylinder actuator.

INTRODUCTION

Author

Advent of the Nuclear Engine for Rocket Vehicle Application (NERVA) created a demand for actuator systems which were simple, reliable, had a minimum of moving parts and sliding surfaces, and which could withstand a high surrounding nuclear radiation field. Based on these requirements, a novel pneumatic stepping motor has been developed by Bendix Corporation under NASA-Lewis Research Center Contract NAS3-5214. This paper describes NASA-Lewis developed flueric logic circuitry to drive the motor and the performance of the breadboard logic circuitry-stepping motor system. Finally a comparison is made

between the pneumatic stepping motor system and the more conventional pneumatic piston actuator.

NOMENCLATURE

A, B, C, D	outputs of counter
$\dot{m}$	mass flow rate
P	pressure
T	timing pulse, torque
t	time
τ	time delay

Subscripts:

a	atmospheric
b	backward
c	control
f	forward
r	receiver
s	supply

Superscript:

$\bar{}$	denotes logical complement of the quantity

STEPPING MOTOR

Shown schematically in figure 1, the actuator motor has only two moving parts: a gimbals supported driving gear free to nutate (wobble) but not to rotate, and an output gear free to rotate but not to nutate. By unequal pressurization of eight bellows attached to its periphery, the driving gear is made to tilt and contact the output gear. As the bellows pressurization pattern is sequenced, the point of contact between the two

gears travels around the circumference of the output gear. Since the output gear has 180 teeth and the nutating gear, 181, the output gear will advance by one tooth, or 2^{o}, for every complete revolution made by the point of contact. If the bellows pressurization pattern, and hence the point of contact, is advanced only a fraction of a revolution, the output shaft will be advanced by the same fraction of 2^{o}. Since eight bellows are used for manipulation of the driving gear, the pressurization pattern can be cyclicly advanced in eight steps and the output shaft position in increments of 0.25^{o}. If the bellows pressurization pattern is fixed at one position, the output shaft position will be also fixed for any load torques less than those which would cause disengagement of the gears. When load torques are applied, a small output shaft deflection occurs accompanied by reverse precession of the nutating gear. However, for torques less than those which cause disengagement, the maximum output shaft deflection will be less than one step size (0.25^{o}). Thus, in the absence of excessive load torques, the actuator motor can accurately position a load at any shaft position specified by sequencing of the bellows pressurization pattern.

Figure 2 and 3 show a section drawing and photographs, respectively, of the motor. To be noted are its inherent simplicity and ruggedness. For a more complete description of the motor and the procedures used in its design, the reader is referred to the contractor's report, NASA CR-54788 (Ref. 1).

BELLOWS DRIVE CIRCUITRY

A requirement of the bellows drive circuitry is to sequence the pressurization pattern at a rate in excess of 160 steps per second. The circuitry originally developed for the motor (ref. 1) was analog and had

feedback paths which detected the position of the nutator gear and fed the correcting signal through two vortex amplifiers in series before it was used. Excessive phase lags contributed by the vortex amplifiers and pneumatic position pickoff appeared to be the main restriction to the circuit's speed (approximately 1/7 of that desired). Accordingly, NASA-Lewis decided to use an open-loop digital counting circuit which was composed of fluid jet devices and which utilized no external position feedback from the actuator.

Figure 4 shows a block diagram of the NASA bellows drive circuitry and acutator motor. The circuitry consists of three main parts: (1) two pulse conditioning units which accept either forwards or backwards directing command pulses and convert them into well defined timing pulses (T_f and T_b); (2) a counter circuit which accepts the timing pulses and converts them into a pressurization pattern stored and advanced on the eight outputs of the counter; and (3) the power amplifiers which take the low power signals delivered by the counter and convert them into high pressure and flow signals for driving the stepping motor. The following sections discuss design aspects of the various circuit components.

Counting Circuit

The counting circuit is a ring type of counter on which is stored a pressurization pattern shifted forwards or backwards by either of two timing pulse trains. Shown schematically by darkened circles in figure 5(a), the required pressurization pattern groups the pressurized bellows next to each other so that maximum force may be exerted on the

point of contact between the nutating and output gears. To be avoided is a pressurization pattern, such as shown in figure 5(b), which shifts the center of force towards the center of the nutating gear and delivers the bellows output force to the gimbals which support the nutating gear rather than to the point of contact between the gears. Thus the counting circuit is required to maintain the pressurization pattern shown in figure 5(a) and sequentially index this pattern around the circumference of the nutating gear, such as shown in figure 5(c).

If the first four bellows are designated A, B, C, and D; the next four $\overline{A}$, $\overline{B}$, $\overline{C}$, and $\overline{D}$; the pressurization of a bellows by the logical state "1;" and the absence of pressurization by the logical state "0;" then table I may be written for the sequencing of the bellows pressurization pattern as a function of the forwards or backwards timing pulses.

If the convention is adopted that a transition of A from logical 0 to logical 1 is called a "set" for A (S_A) while a "reset" for A (R_A) implies a command for transition of A from logical 1 to logical 0; forward command pulses are designated by T_f and backward command pulses are designated by T_b; then the set of logical equations shown in table II may be written for the circuit. It should be noted that setting A implies resetting $\overline{A}$ while resetting A implies setting $\overline{A}$. In table II, * denotes a logical AND while + denotes a logical OR.

Two comments should be made regarding the logical equations of Table II. First, the equations were derived using a synthesis procedure described in reference 2 and make use of the fact that only eight of the possible combinations of the four Boolean variables (A, B, C, and D)

represent acceptable pressurization patterns. The resultant Set and Reset equations (minus the error correcting terms) contain a minimum number of terms, thus simplifying circuit design and reducing flow consumption. During application of the timing pulses, four Set and Reset equations are satisfied by any given counter state. However, three of these are redundant and simply instruct a bistable element to remain in the state it is already in. As long as a correct pressurization pattern has been initially stored on the counter, this redundancy does not affect the desired counting sequence and no need exists for error correction.

Secondly, if an incorrect pressurization pattern is inadvertantly stored or created, it will remain incorrect as it propagates around the counter. Thus some type of error correction is necessary to eliminate any mistakes which might develop in the pressurization pattern. Four terms in the logical equations do not contain either forwards (T_f) or backwards (T_b) pulses. These terms are error correcting terms which detect an incorrect pressurization pattern such as shown in figure 5(b), and issue the appropriate Set or Reset signal to eliminate it. At times, these terms will issue a signal when an error does not exist. However, the generation of an additional signal under such conditions is again merely a redundancy which instructs the affected fluid jet amplifier to remain in the state it is already in. Thus, the error correcting term for S_C would issue a Set signal for C during the initial state of the counter in table I even though no error was present. Once the counter had been advanced two steps forward (from T_f - 0 to T_f - 2 in table I), B would be a logical "0" and would cause the error correction term (B*D) in S_C

to also be a logical "0" (i.e., vanish).

The counter circuit which was developed to satisfy the logical equations of table II is shown, schematically, in figure 6. The pressurization pattern is stored and advanced on four central bistable fluid jet amplifiers, designated I, II, III and IV. Their outputs are designated A, $\overline{A}$, B, $\overline{B}$, C, $\overline{C}$, D, and $\overline{D}$ respectively, corresponding to like designated bellows in figure 5. An active two input OR unit is connected to each control port and furnishes its control signals. To the input of each active OR unit is connected the output of an OR unit acting as a passive AND. These units accept the output of one of the other bistable units as a power supply and a forwards (T_f) or backwards (T_b) counting pulse as their control signal. Their output is thus the logical product (AND) of the outputs of the centeral bistable units and the triggering pulse. For example, the input delivered to the bistable amplifier, I, from the passive OR unit, A_1, is a reset for I and is the logical product of the forward pulse, T_f, and the output of D (i.e., T_f*D). Examination of table II shows that this is indeed the condition by which A is reset by a forwards pulse. Careful examination of the circuit will show that the logical equations of table II are satisfied including the error correcting term. The connections which implement the latter are shown as dashed lines.

Operation of the circuit is as follows: Very short timing pulses of one type only (either T_f or T_b) are applied simultaneously to the control ports of the passive AND units. Those AND units whose power nozzles

are pressurized by the outputs of the central bistable amplifiers (I, II, III, IV) will generate output signals of duration approximately equal to the length of the timing pulse. These output signals travel to the control ports of the active OR units, causing them in turn to generate short output pulses. The output signals from the active OR units switch the central bistable amplifiers. The outputs of the central bistable units are delayed an amount of time, τ, before they reach the nozzles of the passive AND units. Thus, if the timing pulse is short and has vanished by the time changes in outputs from the bistable amplifiers reach the power nozzles of the passive AND units, nothing further will happen and the counter will be set for the next timing pulse. The sequence is repeated with the application of each timing pulse T_f or T_b.

Pulse Conditioning Unit

To furnish the short timing pulse required by the counter circuit, the pulse conditioning unit, shown schematically in figure 7, was used. As illustrated in figure 7(a), the command pulses delivered to the actuator system can be highly distorted as a result of propagating down a long transmission line and will have lower amplitude, rounded leading edges, and long tails. Thus, the function of the first two elements, numbers 1 and 2, in the circuit of figure 7(b), is to shape the ill defined command pulse into one with fixed amplitude and sharp leading and trailing edges. The output of the pulse shaping network is then fed into a unit which fixes the width of the pulse at 1 millisecond. This width is considered to be the minimum value compatible with the switching response of the passive AND units of the counter and the dispersive effects of the lines used

to distribute the timing pulse. Pulse width fixation is accomplished by introducing the command pulse simultaneously to an orifice which feeds control port number C1 of amplifier number 3 and to a 1 millisecond delay line connected to control port number C2 of the same amplifier. Thus, the reshaped command pulse will initially cause flow to go through the number C1 control port, set the amplifier, and produce an output on the R2 receiver. The same command pulse, however, propagates along the transmission line and, 1 millisecond later, pressurizes the number C2 control port. If the pulse delivered by the delay line is of proper magnitude, the number 3 amplifier will be reset and the flow from its R2 receiver shut off, thus terminating the timing pulse. The remaining bistable amplifier, number 4, serves to amplify the pulse in pressure and flow and send it to a manifold for distribution to the control ports of the passive AND units of the counter.

Power Amplifier

The Lewis SB1 power fluid jet amplifier was used to drive the bellows of the nutator motor. Shown in outline form in figure 8, the amplifier has a supersonic nozzle to create the main power jet and uses a conventional, inclined wall interaction region for deflection of the jet. The receivers are of the "Y" type and follow the design philosophy used on the Lewis Model 7 subsonic bistable amplifier (ref. 4). Reverse discharge and displacement flows delivered by the bellows are thus dumped to atmosphere through the vent V_3 instead of into the interaction region. As pointed out in reference 4, this feature permits more rapid switching at lower control port pressures and flows than would be obtained

with a fluid jet amplifier using conventional receivers aimed at the interaction region. A penalty in pressure recovery associated with amplifiers using the "y" type of receivers is felt to be offset by their increased switching speeds and lower control port pressures.

Salient characteristics of the SB1 amplifier when driving the bellows are listed below in table III. To be noted are the short bellows charging time constant of 0.008 second and the rather large internal volume which the amplifier must drive. Figure 9 shows an oscilloscope trace of the bellows pressure as a function of time when the actuator is stepping at maximum rate. As can be seen, the experimental time constant is close to the theoretical, indicating validity of the procedures used to predict the bellows charging times and, hence, the required amplifier size.

BREADBOARD ACTUATOR SYSTEM

To establish the practicality of the previously discussed circuits for the bellows drive circuitry, the circuitry was implemented, in breadboard form, and connected to the stepping motor to form a complete breadboard actuator system. The resultant system is shown in figure 10 and its design performance specifications are listed in table III.

Breadboard Bellows Drive Circuitry

The breadboard implementation of the bellows drive circuitry was made using standard, commercially available fluid jet amplifiers. The fluid jet amplifiers were made of photo-etched ceramic and had barbed hose fittings for input-output connections. All OR units

(including those acting as passive ANDs) were of the asymmetrical wall attachment type and had a power nozzle 0.010- by 0.040 inch. The central bistable units (I, II, III, and IV) of the counter and the bistable units of the pulse conditioning unit were symmetrical wall attachment units, the former having a power nozzle 0.020 by 0.080 inch and the latter, a power nozzle 0.010 by 0.040 inch. Figure 11 shows the manufacturer's silhouettes for the elements and photographs of the units as delivered.

Figure 12 shows a photograph of the pulse conditioning unit. The actual design of the breadboard pulse conditioning unit, especially the input orifice and delay line of the pulse width fixation portion, is somewhat involved and is covered in more detail in reference 3. Figure 13 shows typical output pulses delivered by the pulse conditioning unit into an acoustically terminated, 1/8-inch i.d. line. The 6.0 psig supply pressure listed in the figure is the conditioning unit supply pressure necessary for it to drive the passive AND units of the counter. To be noted are the sharp rise and fall times of these pulses, their repeatability, and their width of 1 millisecond.

A photograph of the counter circuit is shown in figure 14. Each central bistable unit (I, II, III, and IV) with its associated OR-NOR units forms a single layer of seven elements. Four such layers are stacked on top of each other to form the complete counter circuit. A manifold is used to distribute the timing pulses, T_f and T_b, as received from the outputs of the pulse generator. The output of the central bistable amplifiers is fed to junction manifolds located at the control ports of the power

amplifiers. From the control ports of the power amplifiers, the output signals from I, II, III and IV are fed back to the supply nozzles of the various passive AND units in the counter circuit proper.

Two details of the counter design should be pointed out. As noted in reference 3, the steady state viscous pressure losses in a line, for constant mass flow and length, will vary inversely as with the line diameter raised to the fourth power. Thus, motivation exists for using the largest possible line diameter that is consistent with maintenance of the desired delivered pulse wave forms. To distribute the timing pulse to the control ports of the various passive and units, a line of larger internal diameter than optimum was deliberately used. The line's characteristic impedance, however, was such that the reflected wave from it was almost completely terminated by the output impedance of the pulse conditioning unit. Using techniques described in reference 3, it was possible to show that the initial part of the pulse and its peak amplitude should be close to that which would have been delivered by a properly sized line. The tail of the timing pulse was somewhat longer than ideal but still satisfactorily short. Theory was confirmed by experiment as shown by figure 15, which is an oscilloscope trace of the timing pulse as received at the control port of one of the passive AND units. To be noted are the height and width of the pulse as compared to the ideal value.

A similar procedure was used to reduce frictional losses on the carry signals delivered to the power nozzles of the passive AND units. A large (1/8 in. i.d.) line was used to transport the output of the central bistable units to the control ports of the power amplifiers. Part of the flow

was consumed by the control ports of the power amplifiers and the rest was sent down smaller 1/16 inch i.d. lines to the power nozzles of the passive AND units. The latter lines were again somewhat oversized to achieve lower steady-state pressure losses and to permit the use of easily manipulated, flexible rubber tubing. Cancellation of the reflected pulse by the receiver impedance of the central bistable amplifier was very good and, as shown by figure 16, a clean, sharply rising pressure signal with no reflections (D delayed) could be delivered to the power nozzles of the passive and units. Figure 17 shows typical oscillograph traces of the counter output for input rates of 28.7 pulses per second and 173 pulses per second using a counter supply pressure of 12.0 psig.

EXPERIMENTAL PERFORMANCE OF THE BREADBOARD ACTUATOR SYSTEM

To determine the extent to which the breadboard actuator system met the performance specifications listed above, a series of performance tests were conducted. Instrumentation consisted of piezo-electric pressure transducers to measure line pressures at various points in the circuitry and a precision potentiometer to read out shaft position. Static load torques were applied by hanging weights from a line wrapped around a large pulley mounted on the output shaft. Estimated instrumentation errors are:

Pressure	±0.1 psi
Shaft Position	±1/4 percent nonlinearity
Load Torque	±0.10 in.-lbf

Of primary importance was the actuator's maximum slewing rate. As

shown in figure 18, it could be stepped in either direction at 173 steps per second. Rather small, periodic wiggles occurred on the otherwise smooth output trace however. To investigate the source of the wiggles, the actuator was steeped at slower speeds and photographs made of oscilloscope traces of the shaft position. As shown in figure 19, the step sizes are non-uniform. Once every eight steps, a large step of approximately 0.4^{o} occurs. As the stepping rate is increased, the smaller steps become smoothed out but the large step remains as a wiggle. The actuator was disassembled and inspected for obvious flaws, such as dirt between the gear teeth or damaged bellows, which might cause such a change in step size. None were found and the cause of the uneven steps remains unexplained.

Analogous to the frequency response test performed on proportional actuators, the stepping motor can be commanded to cyclicly reverse direction after a fixed number of steps. As shown in figure 20, the inertially loaded actuator system can be cyclicly stepped eight steps (2^{o}) in each direction, without missing, at a stepping rate of 115 steps per second. This performance is roughly comparable to a bandwidth of 7.2 cps for a conventional piston actuator.

Maximum output torque was measured by increasing the load torque on the actuator's output shaft until the driving gear would disengage as the actuator was stepped. The results, shown in figure 21, indicate a maximum static output torque of 70 in. -lbf and a maximum slewing rate of approximately 37^{o} per second. The reduction in output torque from the design value of 103 in. -lbf can be attributed to the inherent

stiffness of the bellows and driving gear gimbal flexures. Since the motor was originally designed to operate with a 70 psid bellows pressure, bellows and gimbal bearing stiffness become significant at the 18 psid bellows pressure delivered by the breadboard circuit. Four psid bellows pressure, alone, was required to force the nutating gear into contact with the output gear. If this pressure is subtracted off the 18 psid pressure experimentally delivered by the breadboard power amplifiers and then divided by the 20.5 psid design value for the breadboard circuit (table III), the predicted reduction in output torque becomes

$$\eta = \frac{18.0 - 4.0}{20.5} = 0.685$$

which is approximately that observed. This reduction indicates an experimental output torque of $T = 0.685 \times 103 = 70.5$ in.-lbf. Thus, for a prototype bellows drive circuitry operating at the NERVA supply and exhaust pressures of 200 psia and 50 psia, respectively, the bellows drive pressures, on the basis of linear scaling of pressures, would be 61.5 psid and the output torque should rise to 82 percent of its design value.

The reduction in maximum, unloaded slewing velocity observed in the torque-speed tests has not been explained but is believed to result from dynamic interactions between the very large pulley used for applying torques to the actuator and the inherent output stiffness of the actuator. When the rated load inertia of 28 lbm-in.^{2} was replaced on the actuator's output shaft, the actuator could again be operated in both directions at 43° per second or 173 steps per second (shown as a dotted square in fig. 21).

COMPARISON OF THE BREADBOARD NUTATOR ACTUATOR SYSTEM WITH A CONVENTIONAL PISTON ACTUATOR

Although the nutator actuator system has a unique set of characteristics which make it inherently well adapted to some applications and less well adapted to others, it is instructive to compare it with the more conventional piston actuator. The method of comparison is to analytically design a frictionless, pneumatic piston actuator, driven by a flapper valve, whose theoretical performance is at least equal to that of the ideal performance of the breadboard actuator system (table IV). The flow required for the actuator systems, their maximum output torques and their maximum slewing velocities are then taken to be the criteria of comparison. Two cases are considered for the stepping motor system: the first is with a power amplifier load volume equal to that calculated for the breadboard actuator system (0.576 $in.^3$), the other with a power amplifier load volume equal to the bellows load volume of 0.237 $in.^3$ plus the internal volume of a channel 1/16 inch square by 7.5 inches long. The latter volume is considered to be the minimum practical manifolding volume that could be obtained in a prototype actuator system. The flow required by the prototype nutator system was determined by first computing the flow required by the power valves and then scaling the rest of the logic circuitry flow in proportion to the power valve flow.

The results are summarized in table V. As can be seen, the primary disadvantages of the stepping motor system are flow consumption and maximum slewing speed. The breadboard system consumes 5.9 times as much flow as an equivalent piston actuator while the prototype system consumes 2.9 times as much. It is possible to further reduce flows

required by the prototype system if: (1) higher pressure recovery power valves are used thus permitting smaller bellows: (2) the bellows stiffness is reduced, thus permitting the same output torques for a lower power valve supply pressure; (3) if a larger bellows charging time constant can be allowed, thus permitting smaller power amplifiers: and (4) if either the bellows volume or line manifolding volume is reduced. The last approach could yield large decreases in power amplifier flow consumption since the prototype system's bellows charging flows outweigh the bellows displacement flows by a factor of 8.2. Reduction of the bellows volume, however, will probably be a difficult task since they have already approximately half of their internal volume eliminated by an insert.

Not treated in this comparison but to be considered are the inherently high open loop output stiffness of the nutator motor, its open loop stability, and the fact that it can be indexed to and held at a position without the use of an output shaft position transducer and complicated feedback networks.

CONCLUSIONS

It is concluded that the fluid jet amplifier bellows drive circuitry is sufficiently fast that bellows charging time is the primary limitation to the maximum stepping motor system speed. Although it has not been tested at higher rates, it is believed that the current bellows drive circuitry can operate satisfactorily at well above 173 steps per second.

It is also concluded that the improved bellows drive circuitry and the stepping motor constitute a reliable, open-loop stepping actuator system

with inherently high output stiffness, reasonable slewing speeds, and small step size. Further improvements in both the actuator and the power valves of the bellows drive circuitry should increase system performance beyond that reported in this paper.

Finally, it is concluded that the stepping motor system's flow consumption will always be much higher than that of an equivalent flapper valve driven piston actuator designed to do the same job. However, for many aerospace applications, this disadvantage in flow consumption may not be large in comparison to the advantages in simplicity, apparent reliability, and high output stiffness that are offered by the pneumatic stepping motor in combination with a flueric digital drive system.

REFERENCES

1. G. R. Howland, "Pneumatic Nutator Actuator Motor," Report Number BPAD-863-16719R (NASA CR-54788), Bendix Corporation, October 17, 1965.
2. W. E. Gromen, "A Transition Map Method of Counter Synthesis," Report Number EDC 1-65-35 (NASA CR-61056), Case Institute of Technology, 1965.
3. W. S. Griffin, "A Breadboard Flueric Controlled Pneumatic Stepping Motor System," Proposed NASA Technical Note.
4. W. S. Griffin, "Design of a Fluid Jet Amplifier with Reduced Receiver - Interaction-Region Coupling," Technical Note D 3651, NASA, October, 1966.

5. K. N. Reid, Jr., "Static and Dynamic Interaction of a Fluid Jet and a Receiver-Diffuser," ScD Thesis, Massachusetts Institute of Technology, September, 1964.

6. F. T. Brown, "Pneumatic Pulse Transmission with Bistable-Jet-Relay Reception and Amplification," ScD Thesis, Massachusetts Institute of Technology, May, 1962.

7. P. Blaiklock and R. Sidel, "Development of a Pneumatic Stepping Motor System", Summer Course Notes 2.73, Massachusetts Institute of Technology, Department of Mechanical Engineering, July, 1966.

TABLE I. - SEQUENCING OF PRESSURIZATION PATTERN

Forward pulse T_f	Backward pulse T_b	Bellows							
		A	B	C	D	$\overline{A}$	$\overline{B}$	$\overline{C}$	$\overline{D}$
0	0	1	1	1	1	0	0	0	0
1	0	0	1	1	1	1	0	0	0
2	0	0	0	1	1	1	1	0	0
3	0	0	0	0	1	1	1	1	0
4	0	0	0	0	0	1	1	1	1
5	0	1	0	0	0	0	1	1	1
6	0	1	1	0	0	0	0	1	1
7	0	1	1	1	0	0	0	0	1
8	0	1	1	1	1	0	0	0	0
0	0	1	1	1	1	0	0	0	0
0	1	1	1	1	0	0	0	0	1
0	2	1	1	0	0	0	0	1	1
0	3	1	0	0	0	0	1	1	1
0	4	0	0	0	0	1	1	1	1
0	5	0	0	0	1	1	1	1	0
0	6	0	0	1	1	1	1	0	0
0	7	0	1	1	1	1	0	0	0
0	8	1	1	1	1	0	0	0	0

TABLE II. - LOGICAL EQUATIONS FOR THE COUNTER CIRCUIT

$$S_A = T_b{*}B + T_f{*}\overline{D} + B{*}\overline{D} = R_{\overline{A}}$$

$$R_A = T_b{*}\overline{B} + T_f{*}D + \overline{B}{*}D = S_{\overline{A}}$$

$$S_B = T_b{*}C + T_f{*}A = R_{\overline{B}}$$

$$R_B = T_b{*}\overline{C} + T_f{*}\overline{A} = S_{\overline{B}}$$

$$S_C = T_b{*}D + T_f{*}B + B{*}D = R_{\overline{C}}$$

$$R_C = T_b{*}\overline{D} + T_f{*}\overline{B} + \overline{B}{*}\overline{D} = S_{\overline{C}}$$

$$S_D = T_b{*}\overline{A} + T_f{*}C = R_{\overline{D}}$$

$$R_D = T_b{*}A + T_f{*}\overline{C} = S_{\overline{D}}$$

TABLE III. - SPECIFICATIONS OF THE LEWIS SB1 POWER AMPLIFIER

Power nozzle throat size	0.040 in. wide by 0.060 in. deep
Design supply to exhaust pressure ratio	4.0
Maximum normalized receiver pressure $(P_r - P_a)/(P_s - P_a)$	40 percent of supply
Maximum normalized receiver flow $(\dot{m}_r)/(\dot{m}_s)$	80 percent of supply
Mach number of power nozzle	1.63
Design load volume	0.576 in.^{3}
Charging time of load volume	0.008 sec
Control port switching pressure $(P_c - P_a)/(P_s - P_a)$	0.07
Control port switching flow (m_c/m_s)	0.06

TABLE IV. - DESIGN PERFORMANCE SPECIFICATIONS FOR THE BREADBOARD ACTUATOR SYSTEM

Working fluid	air
Ambient temperature	530^{o} R
Supply pressures	59.5 psia - power valves
	27 psia - counter circuit
	21 psia - pulse generator
Exhaust pressure	14.7 psia - all components
Maximum output torque	103 in. - lbf
Load inertia	28 lbm - $in.^2$
Maximum stepping rate	160 steps/sec
2^{o} peak to peak amplitude response	7 cps
Bellows internal volume	0.237 $in.^3$
Bellows stroke	0.070 in.
Bellows charging time	0.008 sec
Bellows actuating pressure	20.5 psid
Total manifolding volume per bellows	0.339 $in.^3$ (calculated)
Step size	0.25^{o}

TABLE V. - COMPARISON OF THE NUTATOR ACTUATOR SYSTEM WITH AN IDEAL FLAPPER VALVE DRIVEN PISTON ACTUATOR

Design Performance Specifications:	
Working Fluid	Air at 530° R
Supply Pressure	59.5 psia
Exhaust Pressure	14.7 psia
Output Torque	103 in. lbf
Resolution	$\pm 0.25^{\circ}$
Maximum Slewing Rate	40°/sec
Load Inertia	28.0 lbm-in.^{2}
Frequency Response	Flat to 7 cps, 2° peak to peak amplitude
Actual Stepping Motor System Performance:	
Output Torque	70 in. lbf
Resolution	0.25°
Maximum Slewing Rate	43.3°/sec
Frequency Response	7.2 cps, 2° peak to peak amplitude
Hypothetical Piston Actuator Performance:	
Output Torque	103 in. lbf
Maximum Slewing Rate	188°/sec
Frequency Response	7 cps, 2° peak to peak amplitude
Total System Flow Consumptions:	
Piston Actuator	0.00362 lbm/sec (2.89 scfm)
Breadboard Stepping Motor System (0.576 in.^{3} load volume/bellows)	0.0211 lbm/sec (16.9 scfm)
Prototype Stepping Motor System (0.266 in.^{3} load volume/bellows)	0.01035 lbm/sec (8.2 scfm)

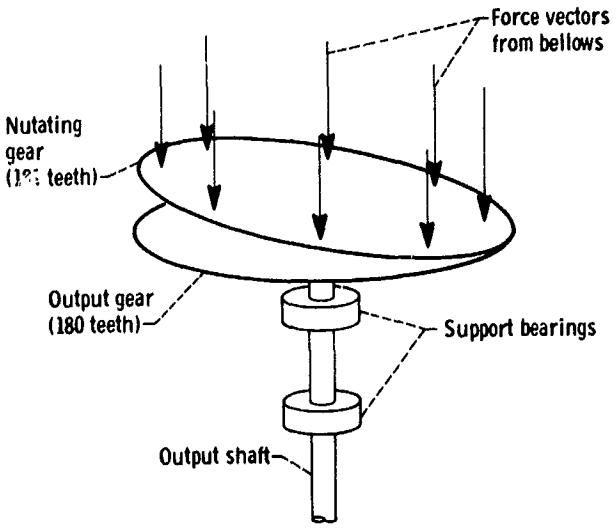

Figure 1. - Schematic of stepping motor operation.

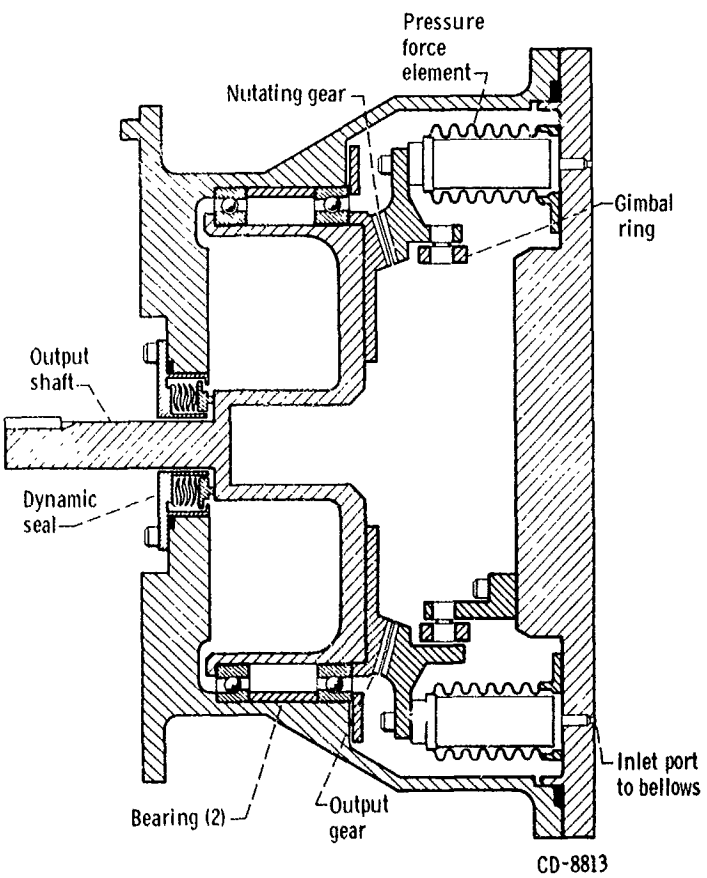

Figure 2. - Cross-section of penumatic stepping motor.

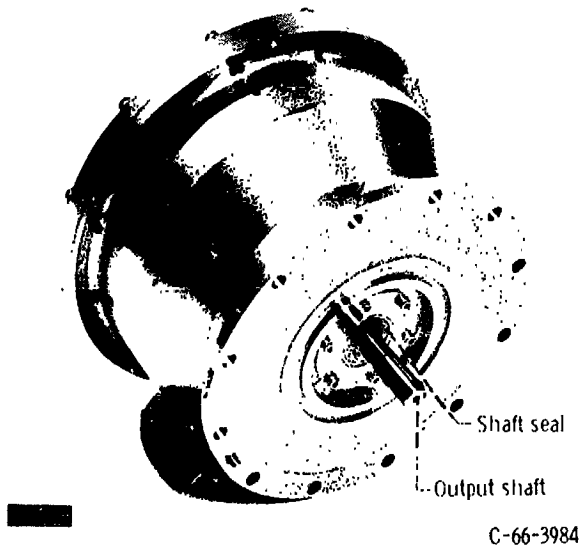

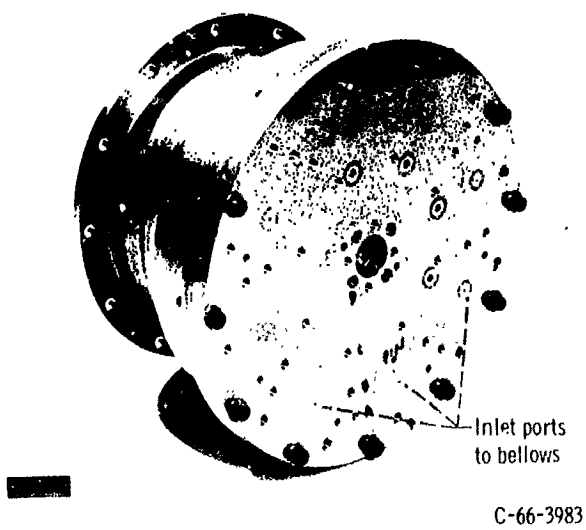

Figure 3. - Stepping motor.

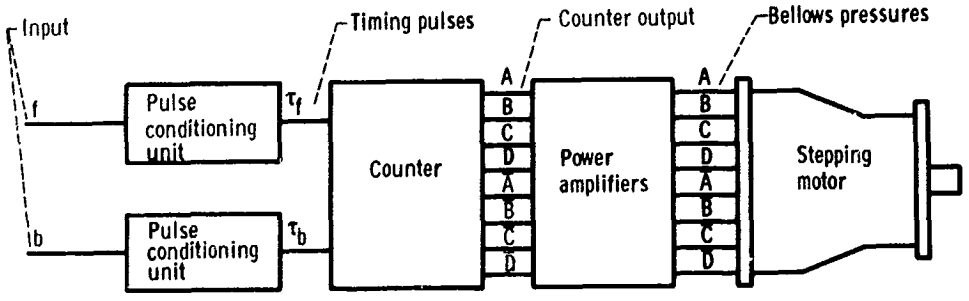

Figure 4. - Block diagram of breadboard actuator system.

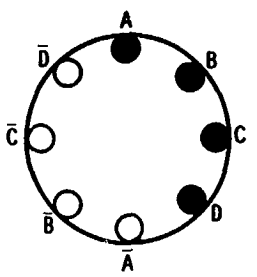

(a) Correct pressurization pattern.

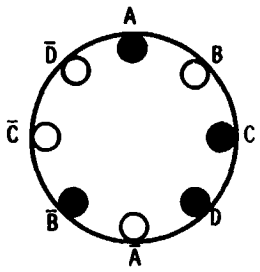

(b) Incorrect pressurization pattern.

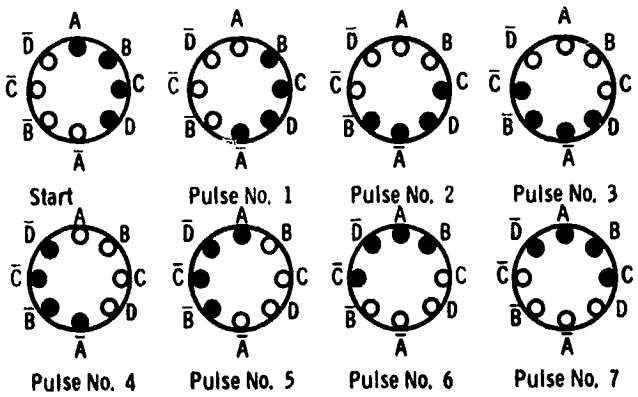

(c) Sequencing of pressure pattern by forward counting input pulses.

Figure 5. - Bellows pressurization patterns.

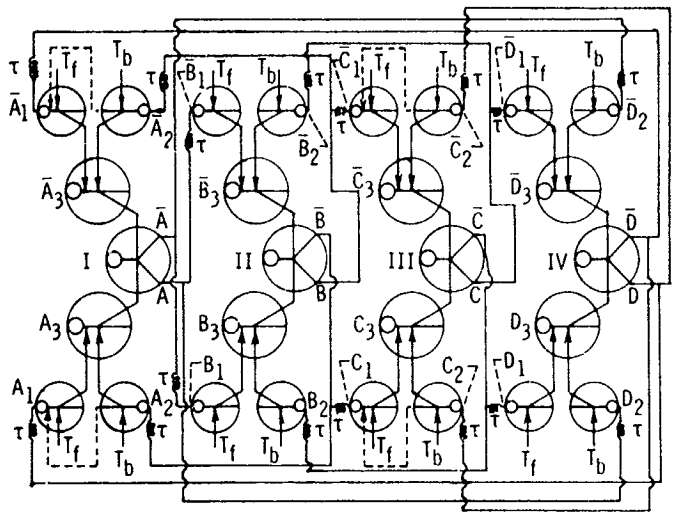

Figure 6. - Schematic of counting circuit for nutator motor.

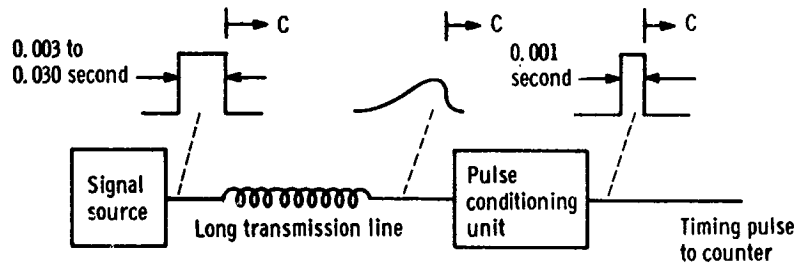

(a) Command pulse wave forms.

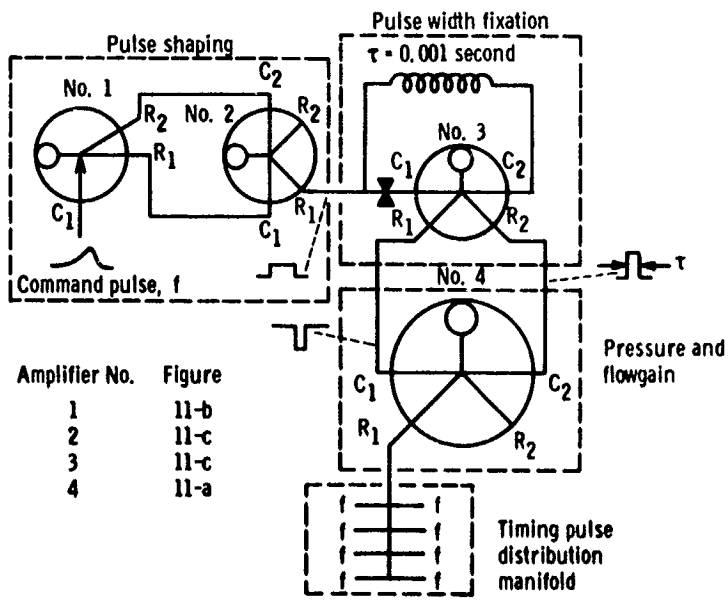

(b) Schematic of pulse conditioning unit.

Figure 7. - The pulse conditioning unit.

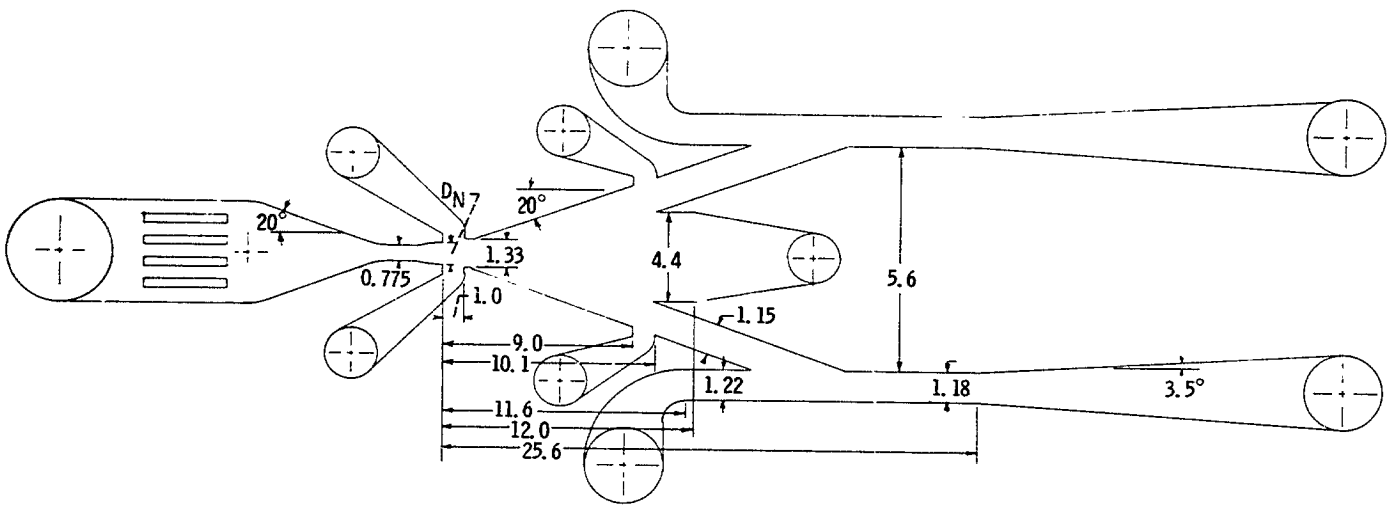

Figure 8. - Lewis SB-1 power amplifier. (All linear dimensions to be multiplied by D_N.)

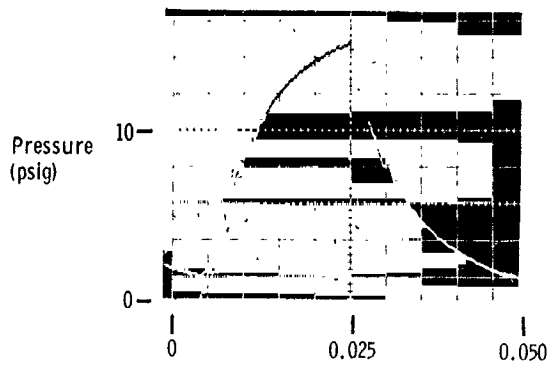

(a) 173 steps/sec.

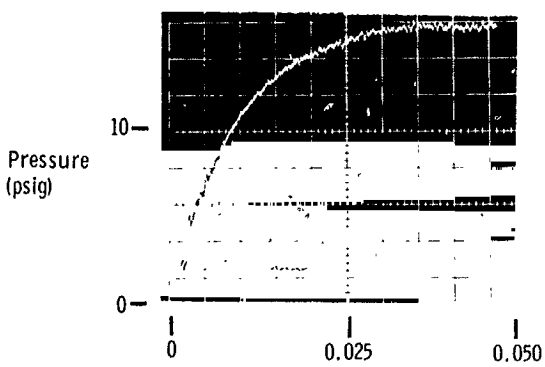

(b) 28.7 steps/sec.

Figure 9. - Bellows pressure versus time.

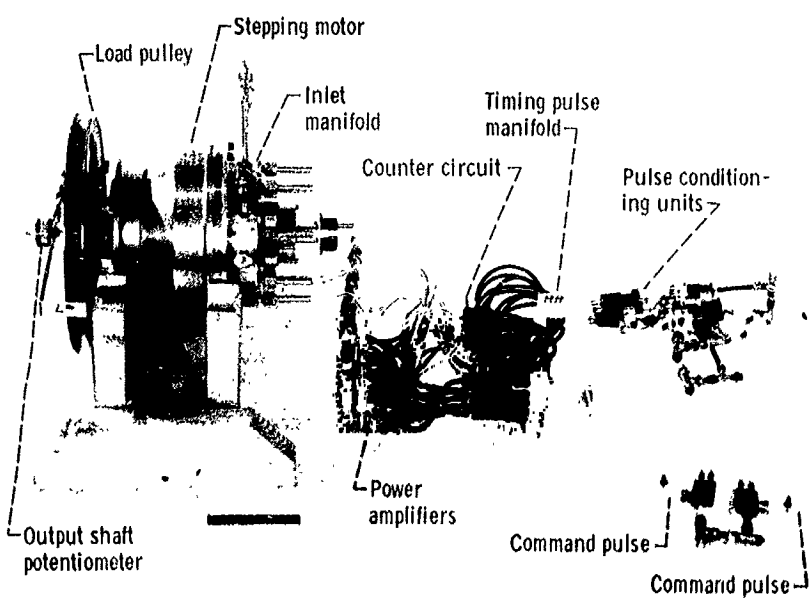

Figure 10. - Breadboard actuator system.

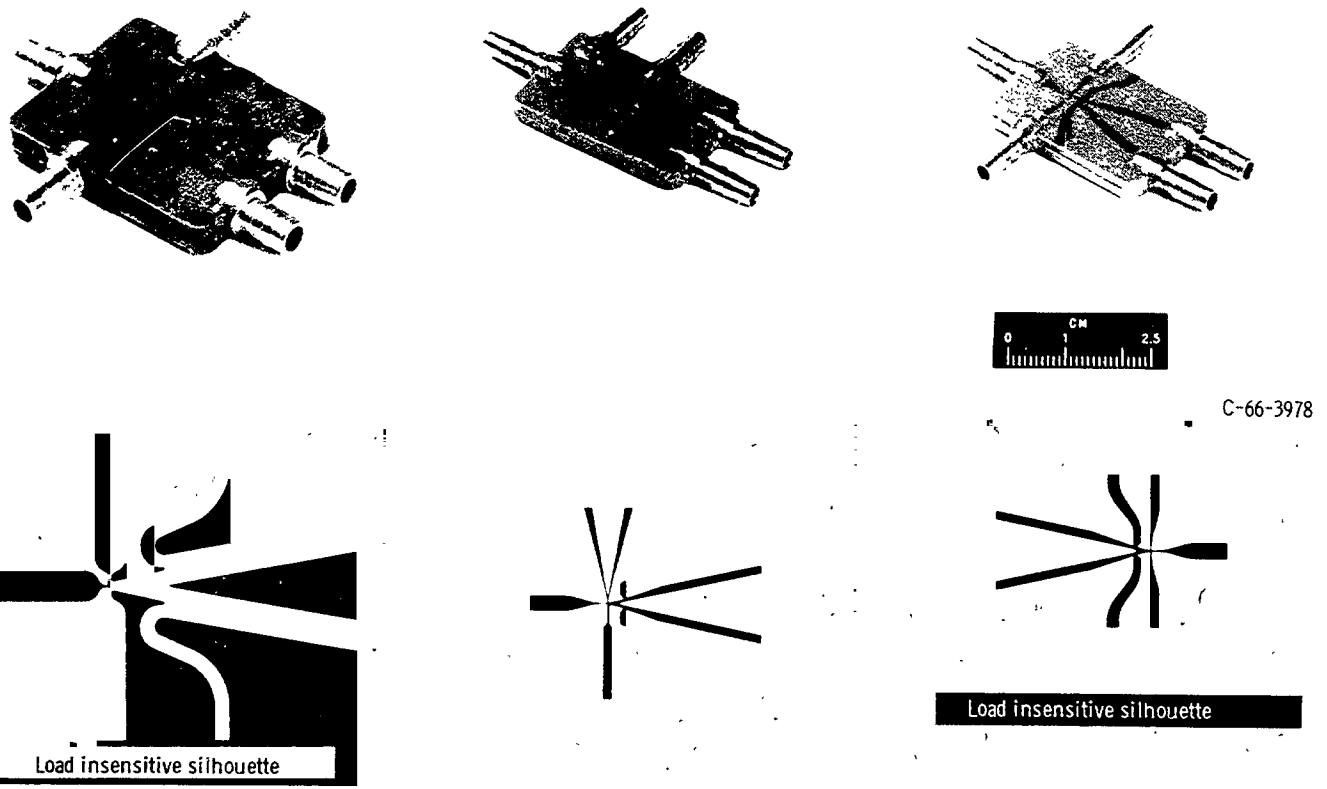

(a) Bistable amplifier (0.020x0.080" power nozzle).

(b) OR-NOR unit (0.010"x0.040" power nozzle).

(c) Small bistable amplifier (0.010"x0.040" power nozzle).

Figure 11. - Pictures and sillouettes of fluid jet amplifiers used in breadboard bellows drive.

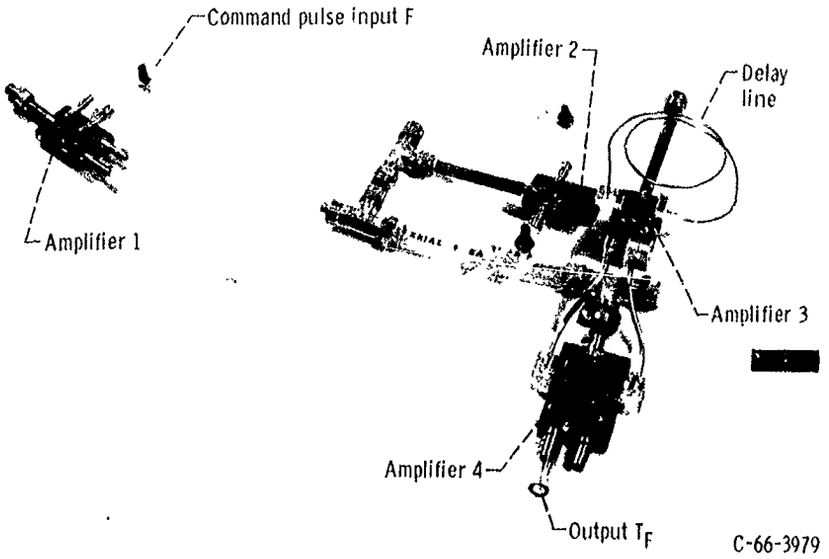

Figure 12. - Pulse conditioning unit.

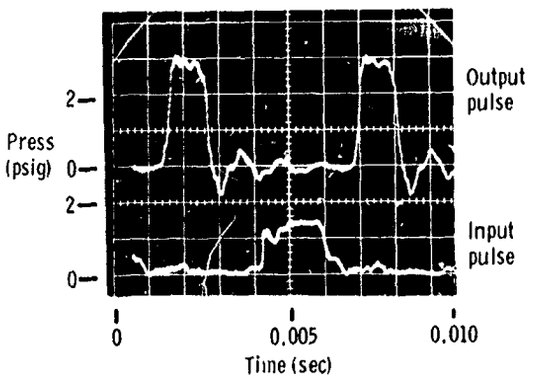

(a) 12.0 psig circuit pressure.

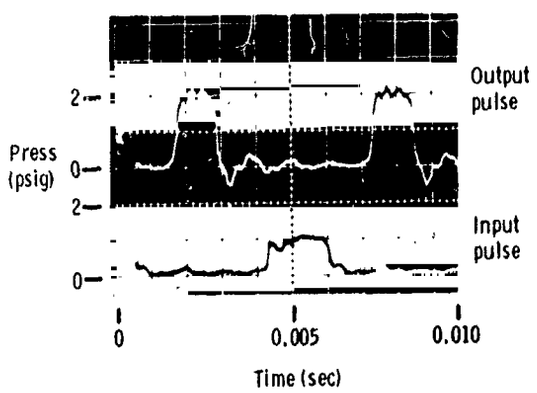

(b) 6.0 psig circuit pressure.

Figure 13. - Output of pulse conditioning unit.

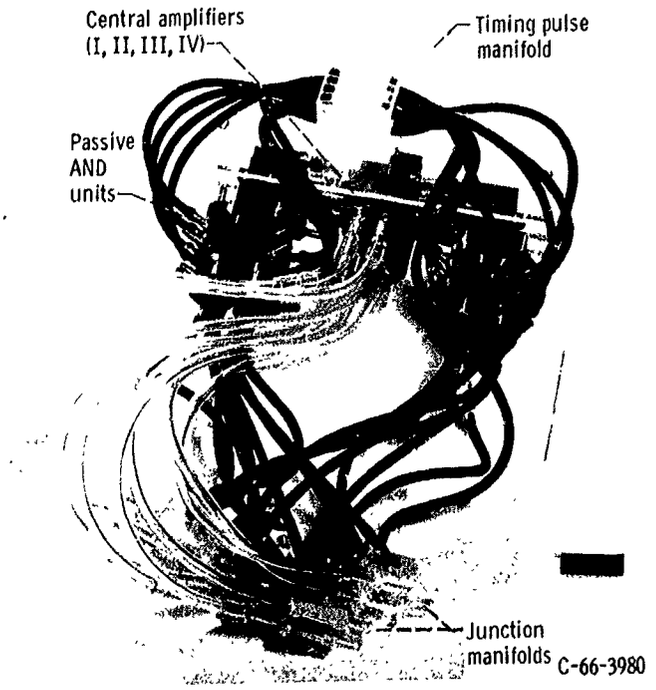

Figure 14. - Breadboard counter circuit.

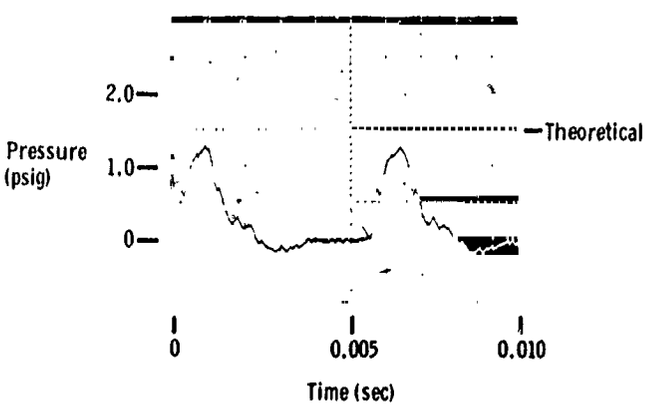

Figure 15. - Timing pulse delivered to control port of passive AND unit. 6.0 psig supply pressure to pulse conditioning unit.

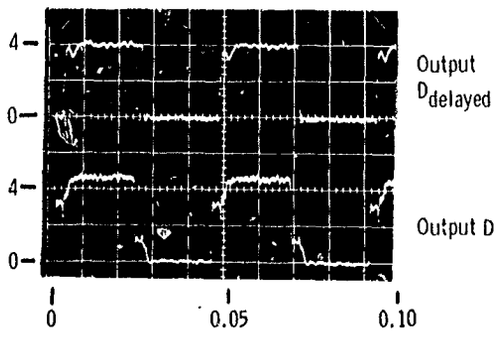

(a) 12.0 psig circuit pressure.

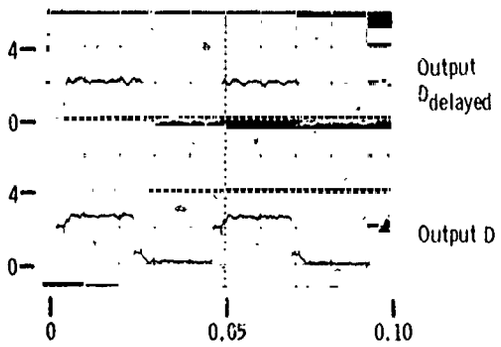

(b) 6.0 psig circuit pressure.

Figure 16. - Counter outputs D and $D_{delayed}$.

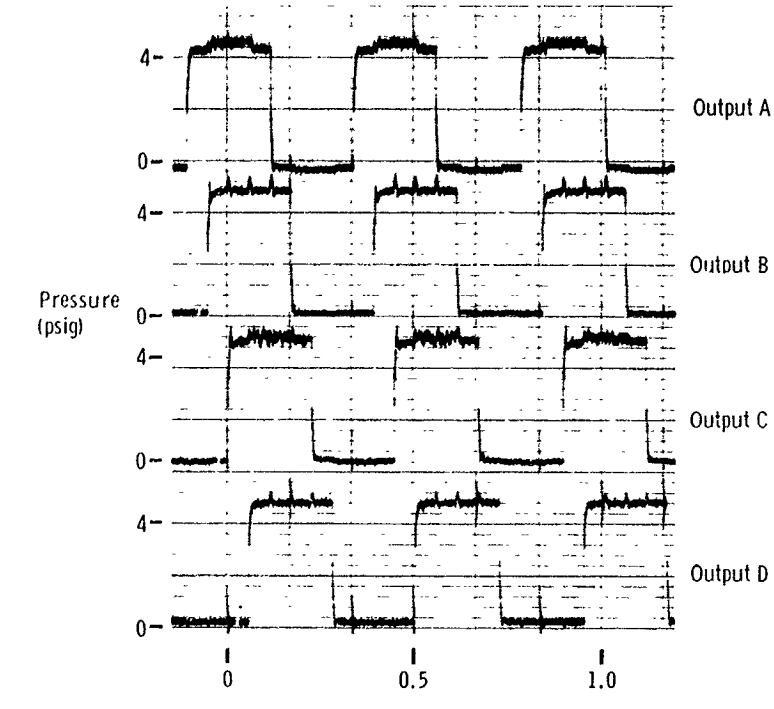

(a) 27.5 steps/sec.

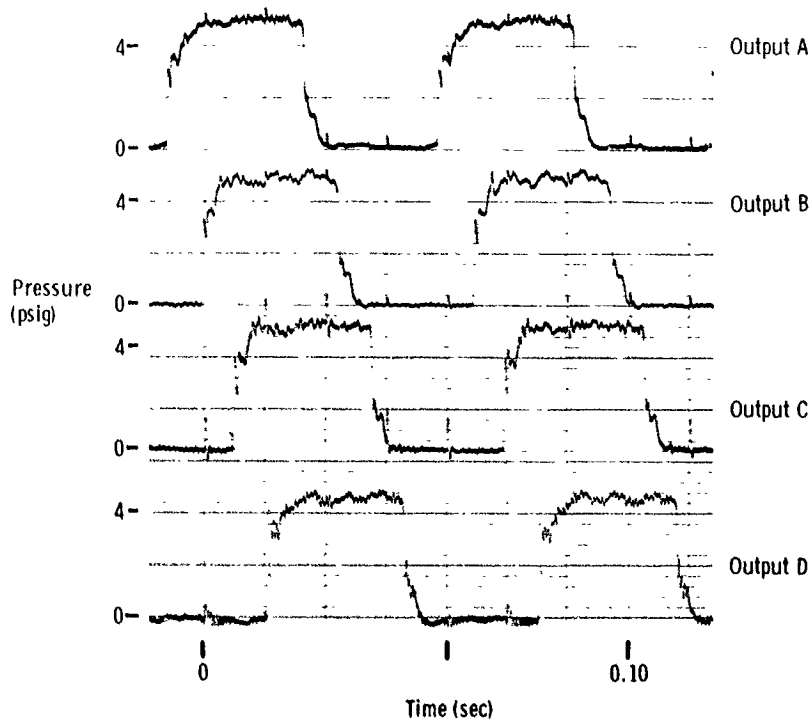

(b) 173 steps/sec.

Figure 17. - Counter outputs

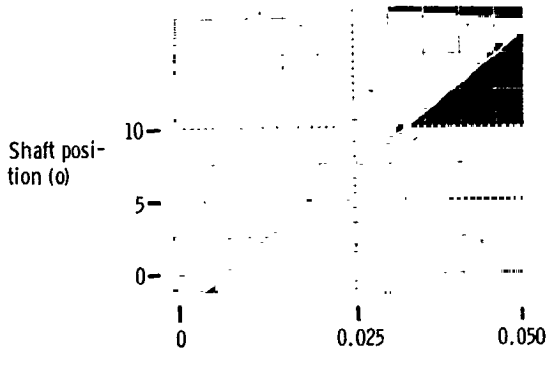

(a) Forward direction.

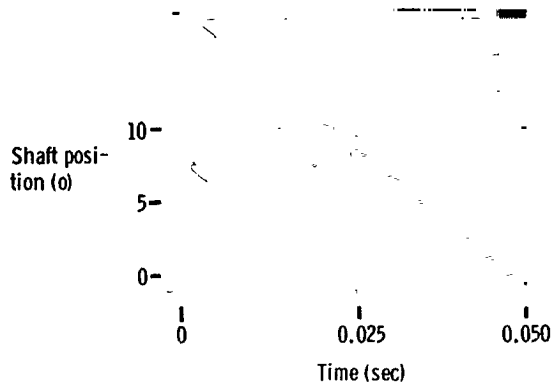

(b) Backward direction.

Figure 18. - Output shaft position versus time - 173 steps/sec.

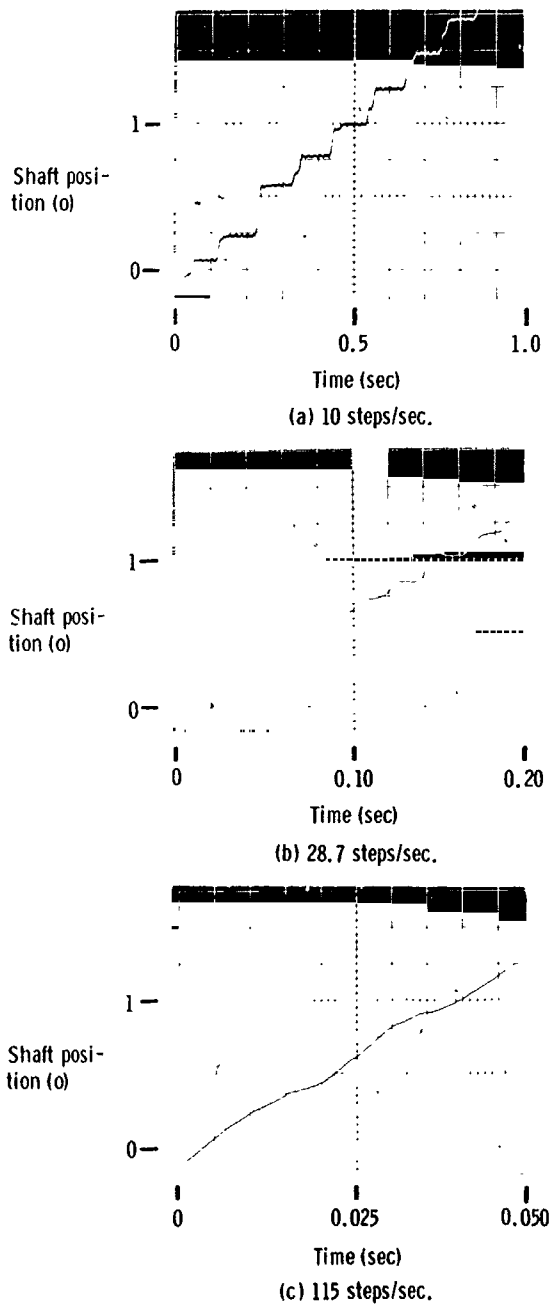

Figure 19. - Output shaft position versus time. Steady stepping rate.

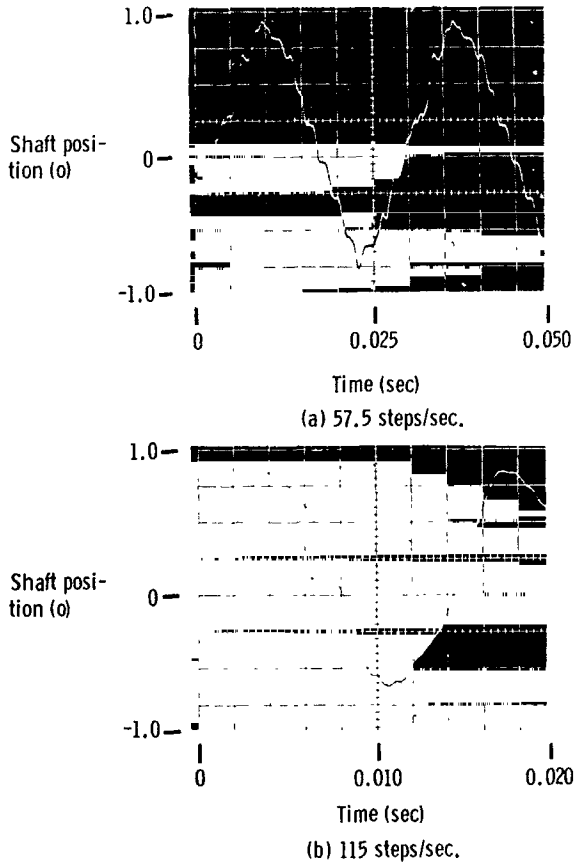

Figure 20. - Small amplitude response of breadboard actuator system. Eight steps each direction.

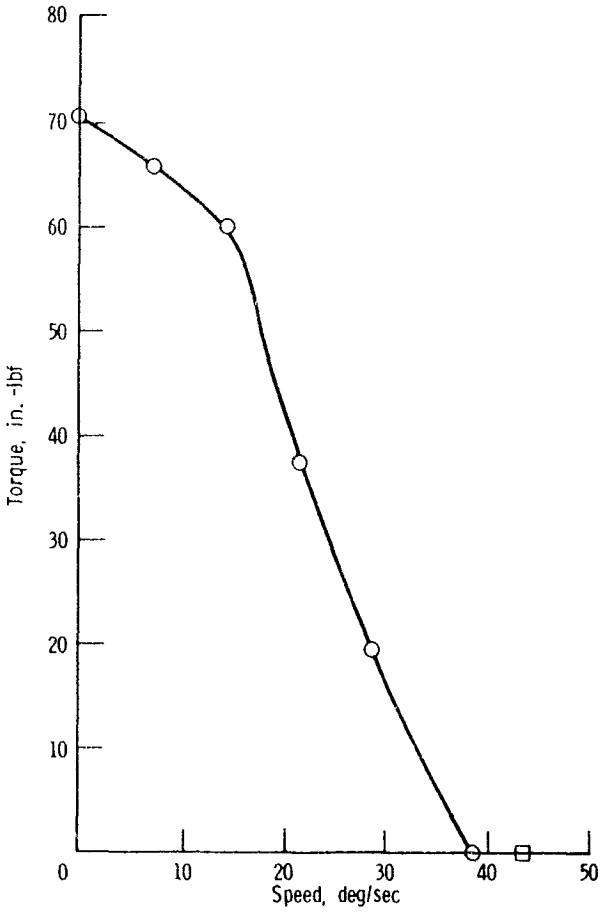

Figure 21. - Output torque against speed of breadboard actuator system.